Proceedings of the
Annual Stability Conference
Structural Stability Research Council
San Antonio, Texas, March 19-22 2024

Elastic post-buckling behaviour of single layer steel reticulated barrel vaults

Vanama Sai Dhanush[1], Raghavan Ramalingam[2]

Abstract

Barrel Vaults are singly curved shell structures common for roofing of long hallways and platforms, spanning along one direction. Steel reticulated barrel vaults consist of several members functioning predominantly by transfer of axial forces. They are susceptible to limit point buckling instability similar to other types of reticulated shells, and exhibit post-buckling behaviour in the elastic range. While research on post-buckling of reticulated doubly curved domes is abundant, that on singly curved barrel vaults is limited. Therefore, the objective of this study is to perform the post-buckling behaviour of single layer barrel vaults for idealistic and practical load cases. The geometric parameters are varied using different span-to-rise ratios, different member cross-sectional areas and different span-to-breadth ratios. The idealistic load cases are concentrated central load, apex line load and uniform pressure load while maintaining the same total magnitude in all 3 cases. To check pratical loading conditions, the same barrel vaults were also analysed with wind loads applied with distribution as per the Indian Standard IS:875-2015 part III. The corotated-updated Lagrangian formulation was used for the postbuckling analysis. The analysis results showed that among all types of loading, uniform pressure leads to the highest elastic critical load for any barrel vault, and the critical loads for practical wind loading conditions generally fall below that of uniform pressure. Among the geometric ratios, span-to-rise ratio is more influential than span-to-breadth ratio. It is also found that there are limiting values to length-to-breadth and span-to-rise ratios beyond which the critical load is fairly unaffected. To address the absence of analytical equations to predict the critical loads, existing equations in literature for cylindrical shells are selected and compared with the results from the analysis.

1. Introduction

Reticulated space structures are a group of three-dimensional structural systems that consist of straight bar elements. They exhibit well-distributed and predominantly axial internal forces. Reticulated structures can be classified based on their geometric forms similar to the classification for solid shells such as, singly or doubly curved, synclastic and anticlastic, geometries of translation or revolution etc. Among the various forms barrel-vaults are singly curved reticulated structures arched in one direction and their bounding surface is generated by translation. The shape of their sections is mostly that of an arc of a circle though elliptical and cycloidal sections are also present. The barrel vaults are commonly used for covering areas that

[1] Junior Engineer, Military Engineering Services, India <saidhanush.vanama@gmail.com>
[2] Assistant Professor, National Institute of Technology Tiruchirappalli, India <raghavanr@nitt.edu>

are longer in one direction such as railway stations, hangars, and industrial sheds and can be constructed in single-layer, double-layer, or multi-layer configurations.

Reticulated barrel-vaults are sensitive to large displacements and display post-buckling behavior similar to that of reticulated domes, involving snap through limit points. Their geometrically non-linear behavior has not received the same attention in literature as that of reticulated domes on which studies are more abundant. Hence, researchers are restricted to refer to studies on reticulated domes and solid cylindrical shells for approximating the stability of these singly-curved reticulated structures. In addition to span-to-rise ratio which is the most significant geometric ratio for reticulated domes, the importance of the span-to-breadth ratio needs to be ascertained for barrel-vaults. Therefore, due to this shortage, studies on the post-buckling behavior of reticulated barrel-vaults is merited.

The works of earlier researchers Papadrakakis (1983), Hill et al (1989), Yang and Yang (1996) in developing geometric and material nonlinear formulations for reticulated domes and solution techniques for overcoming the limit point formed the benchmark for further research on reticulated structures. More efficient solution techniques using calculated minimum residual energy (Jayachandran et al, 2004; Rezaai-Pajand and Alamatian, 2011) and other techniques (Mohit et al, 2020) have been applied to the postbuckling analysis of these structures though the Generalised Displacement Control (GDC) adopted by Thai and Kim (2009) has demonstrated path tracing with computational efficiency. Progressive instability analysis (Jiachuan et al, 2016) and vulnerability analysis (Guibo et al, 2017) have also been studied. The influence of geometric ratios and loading distribution on the elastic critical loads have been ranked by Dara et al (2020) and Jeyabalan and Ramalingam (2022).

The rigidity of the connectors has been investigated as an influencing parameter in the critical load of the reticulated domes (Lopez et al, 2007; Ahmedizadeh and Maleek, 2014; Ramalingam and Jayachandran, 2015; Huihuan et al, 2016) and barrel vaults (Ma et al, 2011), which can significantly alter the deflection computations as well. With regard to literature specific to the behavior of reticulated barrel vaults, El-Sheikh (2007) discussed their sensitivity to geometric imperfections and identified critical locations of the barrel vaults. The work of Ma et al (2011) is unique by being one of limited experimental tests for the stability of cylindrical reticulated vaults. The effects of support settlement (Sheidaii, 2013), out-of-straightness and lack of fit (random distribution study by Roudsari et al, 2017) show that these structures are critical to the accurate prediction of their capacities. While researchers have applied the popular Wright's (1965) formula for estimating the critical snap through loads of domes, a similarly well know equation for estimating for barrel vaults is absent. In light of this, classical equations for solid cylindrical shells by Timoshenko (2009) and those listed by Lo Frano et al (2009) subjected to all round pressure are the ones with available for structures of similar curvature and geometry (except that reticulated vaults are not a full circle in cross-section) that can also undergo shell type buckling under external pressure.

Following from the above discussion on reticulated structures and barrel vaults, the present study is formed with the following objectives:

1.To determine the critical loads and post-buckling behaviour of single layered reticulated barrel vaults under different load patterns viz., concentrated central load, apex line load, uniform pressure and practical wind pressure distributions.
2. To obtain effect of vault's geometric parameters viz., span-to-rise ratio, and span-to-breadth ratio, on the critical load of vault.
3. To compare the predictions by modifying existing analytical equations for the critical load of single layered barrel vaults under different loading conditions.

2. Barrel Vault Models and Parameters

2.1 Geometry parameters

Geometric parameters are fundamental in the global stability and critical load of the reticulated barrel vaults and they are determined through a post-buckling analysis. The generation of the barrel vault geometry and their members are easily done by any structural modelling software by creating a plane arc with nodes and members, creating plan diagonal members and then translating the arc for the required spacing and length. Snap-through load (critical load) and vertical deflection at snap through are the primary results from the elastic post-buckling analysis used to determine the effect of various parameters on global stability.

The geometric parameters used for generation and analysis of the barrel vaults are span-to-breadth (L/B) ratio, span-to-rise ratio and member cross-sectional area. The span is kept fixed while varying the L/B and span-to-rise ratios. These parameters are listed in Table 1. The boundaries of the vault are considered as pinned at the edges along the breadth and along the arc, corresponding to the provision of edge supports and traverses at the ends of the vault. All members are considered as 2-noded axial linear bar elements with 3 degrees of freedom per node and all loads are nodal concentrated loads.

2.2 Load Parameters

All barrel vault models mentioned above are analysed for three different load patterns, and in every case, the total magnitude of the reference load applied on the vault is 600 N (gravity direction). The three different load patterns used for this study are concentrated central load, apex line load, uniform pressure and practical wind pressure distribution. Fig 1 shows the barrel vaults with loads applied as per the above mentioned patterns. The models in the figure from are made in software STAAD.Pro for visualizing though this software is not used for the analysis. The total reference load is divided into multiple concentrated nodal loads according to the load pattern. In case of uniform pressure, the reference load is divided by the total number of nodes in the vault except for the supported nodes. Table 2 lists the data relating the number of nodes and the magnitude of nodal loads applied for each load pattern.

For practical wind pressure distribution, the magnitude of the wind pressure has been calculated with provisions that of the Indian Standard for wind loading, IS:875 (part III) - 2015. Unlike uniform pressure case where the loads are applied vertically along gravity, wind pressure (both positive and negative) acts perpendicular to the surface and the pressure coefficients depend on the span-to-rise ratio. Hence, this perpendicular load is resolved into normal and horizontal load components for application as nodal loads.

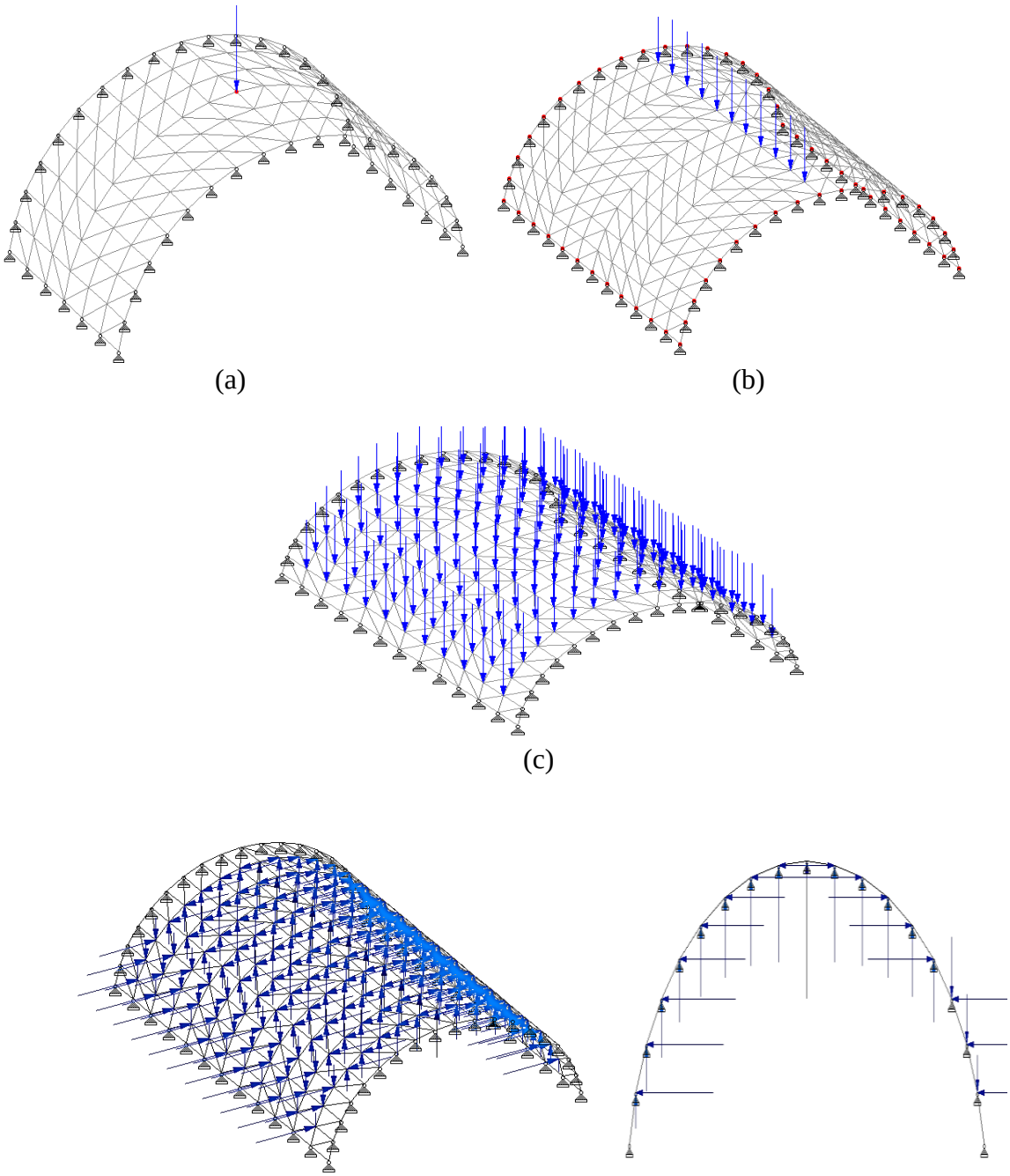

Figure 1: Load patterns used for analysis of the barrel vaults: (a) concentrated central load, (b) apex line load, (c) uniform pressure, (d) practical wind pressure (global view and elevation)

Table 1: Geometric parameters and their values used for vault generation

S.No	Geometric Parameters	Values
1	L/B ratio	0.5, 1, 1.5
2	Span/Rise ratio	2.35, 3.28, 4, 6, 8,10
3	C/S area of member(mm^2)	181, 207, 302, 352, 404, 633
4	Average length of member(*mm*)	1500, 2000

Table 2: Node-Member-Load data for different L/B ratios

		L/B = 0.5	L/B = 1	L/B =1.5
No. of Nodes		133	247	247
No. of Members		348	678	678
No. of Non-supported Nodes		85	187	187
No. of Nodes at crest of vault		5	11	11
Magnitude of Concentrated Load	Point Load	600 N	600 N	600 N
	Line Load	120 N	54.55 N	54.55 N
	Uniform Pressure Load	7.06 N	3.21 N	3.21 N

The wind pressure magnitudes have been calculated using the provisions from IS:875 (Part III) - 2015. For cylindrical roofed structures resembling clad barrel vaults (Fig 2), the external pressure coefficients that are to be followed have been taken from Table-18, Cl.7.3.3.6. These coefficients are dependent on the curvature which is provided in the table by span-to-rise ratio.

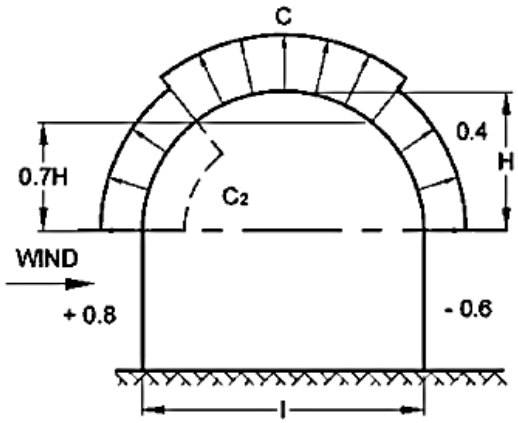

H/l	C	C_2
0.1	-0.8	+0.05
0.2	-0.9	+0.1
0.3	-1.0	+0.15
0.4	-1.1	
0.5	-1.2	

Figure 2: Wind Loading pattern on elevated cylindrical roof structure as per IS:875 (Part III) – 2015

For this study, the following values have been used to calculate the wind pressure by IS: 875 (Part III) – 2015 - basic wind speed (V_b) 47 m/s, probability factor (k_1) 1.0, terrain roughness and height factor (k_2) 1.0, topography factor (k_3) 1.0, importance factor for cyclonic regions (k_4) 1.15, wind directionality factor (k_d) 0.9, area averaging factor (k_a) 0.8, combination factor (k_c) 0.9 and internal pressure coefficients are adopted as ±0.2 corresponding to 5% openings. After wind pressure calculation for the different parts of the vault (C_2, C and the rest, as shown in Fig 2), the pressure is converted to nodal loads by dividing the number of unsupported nodes in each part and resolving into equivalent vertical and horizontal components.

3. Analysis Methodology

3.1 Postbuckling analysis using CR-UL formulation

The corotated-updated Lagrangian (CR-UL) nonlinear formulation (Ramalingam and Jayachandran, 2015) is used in this study for the determination of the critical load and post-buckling paths. Readers are directed to the fundamental work by Mattiasson (1983) and Jayachandran et al (2004) for the mathematic principles of the corotational approach. The key components of the corotational approach involve decomposition of deformations into rigid body displacements and stress producing (natural) deformations and their derivations are discussed in detail in Jayachandran et al (2004). The nonlinear finite element equations, based on the aforementioned deformation components, are derived in the updated Lagrangian formulation by considering the last known configuration as the reference configuration. A depiction of the CR-UL approach is shown in Fig 1.

Eqs 1-6 are equations denoting each step of the CR-UL approach for axial bar elements. The notations are as per Mattiasson (1983)

$$\delta p_n = [-1 \quad 0 \quad 0 \quad 1 \quad 0 \quad 0] \begin{Bmatrix} \delta u_1' \\ \delta v_1' \\ \delta w_1' \\ \delta u_2' \\ \delta v_2' \\ \delta w_2' \end{Bmatrix} \tag{1}$$

$$\delta q = A^T E^T \delta q_n + A^T \delta E^T q_n \tag{2}$$

$$\delta q_n = K' \delta p_n \tag{3}$$

$$K_L = \frac{A}{L}(C + \sigma) \tag{4}$$

$$\delta q = A^T E^T K' E \delta p' + A^T q_n B \delta p' \tag{5}$$

$$\delta q = A^T (E^T K' E + q_n B) A \delta p \tag{6}$$

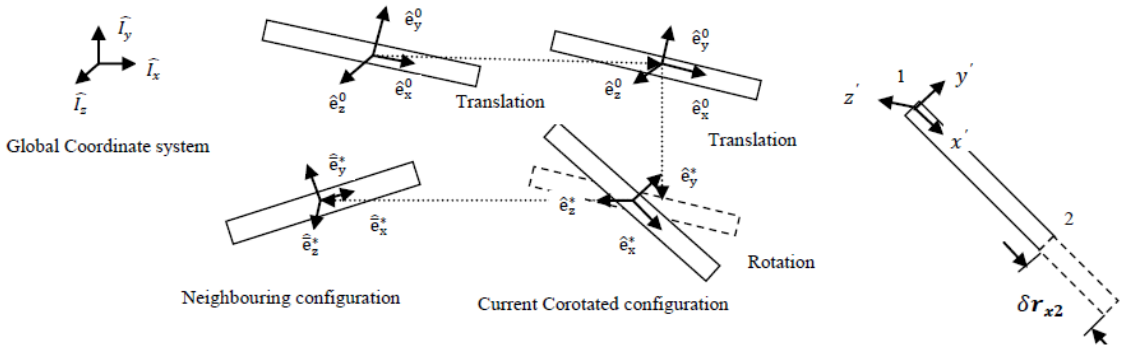

Figure 3: Description of motion in the CR formulation (Jayachandran et al, 2004)

Eqn 1 obtains the natural displacements p_n from the nodal displacements of the current configuration $\delta u_1'$ to $\delta w_2'$, Eqns 2 and 3 show the change in the nodal force vector δq using the change in natural force q_n which is calculated from the natural stiffness K' and natural displacement p_n. The local tangent stiffness thus derived for bar elements is geometric nonlinear and inclusive of the stress σ (Eqn 4). Eqns 5 and 6 are used to calculated the global tangent stiffness $K_G = \delta q/\delta p$, using the natural stiffness K', natural force q_n and transformation matrices from global to local coordinates A and from local to natural coordinates E. The minimum residual displacement method by Chan (1988) has proven to be efficient in overcoming limit points such as snap-through typical of reticulated shells and is used in this program as the solution procedure. The accuracy of the program has been validated in previously published articles and thus validation is not repeated here.

3.2 Analytical Equations in literature for critical load of barrel vaults

The results from the post-buckling analysis that done in this study will be compared with following equations by substituting all geometric parameters. Eqn 7 and 8 are given below are from Cheng and Ho (1963) and Timoshenko et al (2009), but for solid cylindrical shells.

$$P_{cr} = \frac{2\pi E t^2}{3\sqrt{6}(1-\nu^2)^{(3/4)} RL}\sqrt{\frac{t}{R}} \tag{7}$$

$$P_{cr} = \frac{Et}{R(n^2-1)\left(1+\frac{n^2L^2}{\pi^2R^2}\right)} + \frac{Et^3}{12R^3(1-\nu^2)}\left(n^2-1+\frac{2n^2-1-\nu}{1+\frac{n^2L^2}{\pi^2R^2}}\right) \tag{8}$$

where, t is thickness of shell, R is radius of the shell, L is the length of the shell, n is the number of circumferential buckling waves for the buckling mode, E is the Modulus of Elasticity and $\boldsymbol{\nu}$ is the Poisson's ratio. Since the above equations were developed for solid cylindrical shells, these equations cannot be used directly for reticulated barrel vaults. In order to use these equations, an equivalent thickness for the reticulated barrel vault has to be approximated which is done in this case by dividing the total material volume of vault by surface area of vault. The total material volume of vault is the summation of area of each member multiplied by the length of member for all members in the vault. The curved surface area of the barrel vault is calculated as done using

the formula for cylinders. Another major difference is that the pressure on the cylindrical shell acts all around the circular cross-section. For the barrel vault, there are two longitudinal edges which are supported in addition to the curved ends, while for the cylindrical shell only the ends faces would be closed and supported,

4.0 Results

4.1 Effect of load pattern on critical load and shape of postbuckling curve

The distribution of the load over the entire surface of the barrel vault has a large effect on the critical load and post-buckling behavior. Since the barrel vaults are symmetric, under symmetric loading conditions, snap through at the apex is the most common instability that occurs. Following the post-buckling analysis of all the vaults, for all the load patterns, comparisons have been made graphically. Though most literature on reticulated structures study snap-through instability with concentrated crown loads on domes, this represents an extremely conservative and impractical case. Very early instability is predicted when large and sharp loads are applied on a node as compared to the same magnitude of load distributed across the surface of the structure. Fig 4, shows the load factor vs apex node deflection for the barrel vault with L/B ratio 1.0, span-to-rise ratio 2.35 for different member cross-sectional areas. In the figure, the upper bound of the load factor axis is set to the load factor obtained for uniform pressure case. The solid curves corresponding to apex line load are observed clearly. For clarity, the curves for point central load and uniform pressure are in-set within the same graph.

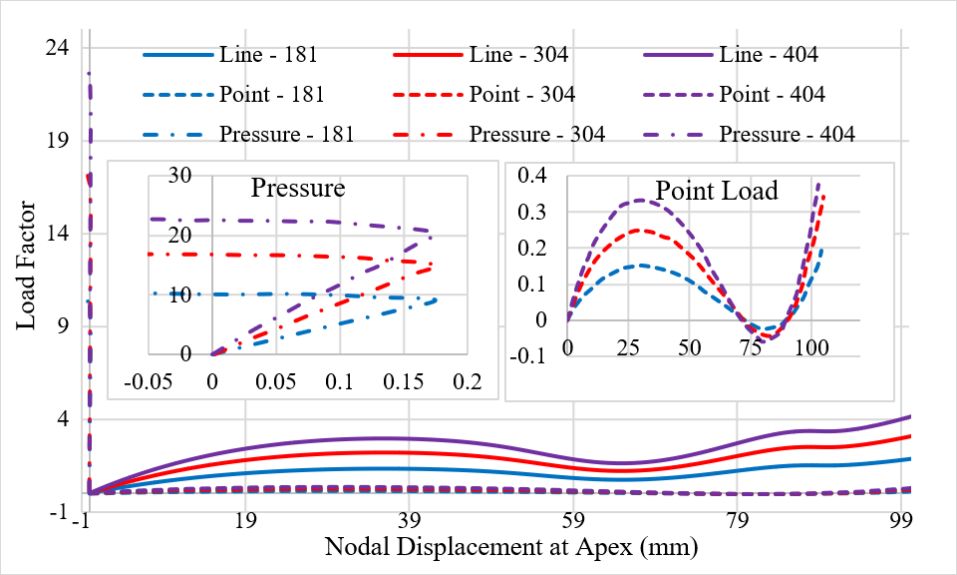

Figure 4: Load factor vs apex node deflection of barrel vaults with different member cross-sectional areas under three different symmetric load patterns

As per expectation, for the same total load magnitude, uniform pressure distribution leads to a significantly higher critical load. As seen from the in-set plot, the post-buckling curve does not follow snap-through and the apex node undergoes reversal (uplift) due to the geometric changes to keep up with the displacements caused by the loads on adjacent nodes. This trend in shifting the critical mode away from snap-through can also be judged from the load-deflection curves of the apex line load case. The snap-through curve in this case does not cross into the unloading (negative load factor) and the snap-through action is much gradual. This is in contrast with the

familiar snap-through curves seen for the classical 'toggle truss' and pin supported reticulated domes, as well as the central point loaded barrel-vault (in-set plot). Fig 5 shows the deflected shape of the barrel vault under uniform pressure at the critical load factor.

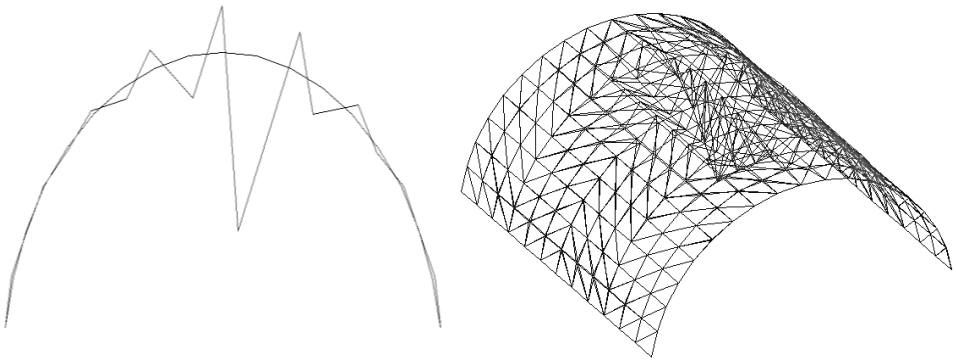

Figure 5: Deflected shape of barrel vault subjected to Uniform Pressure load

4.2 Effect of span-to-rise ratio

The span-to-rise ratio is known to be the most important parameter influencing snap-through in both reticulated and solid shell structures. The effect on reticulated barrel vaults is displayed in Fig 6(a) with apex line load for L/B ratio 0.5 and cross-section area of member 404 mm^2. The figure shows the significance of the span-to-rise ratio and limit points subsequent to snap-through are also denoted by the solid circles. The snap-through curves do not have any portion in the negative load factor ranges for the chosen L/B ratio of 0.5. The fall in the first (snap-through) critical load as the span-to-rise ratio increases is depicted in Fig 8 under uniform pressure load. A huge drop in critical loads above span-to-rise ratio of 4 is seen in both Fig 6(a) and Fig 8. From a design perspective this can be compared with the commonly adopted span-to-rise ratios of 6-8 for reticulated domes for safeguarding against snap-through instabilities.

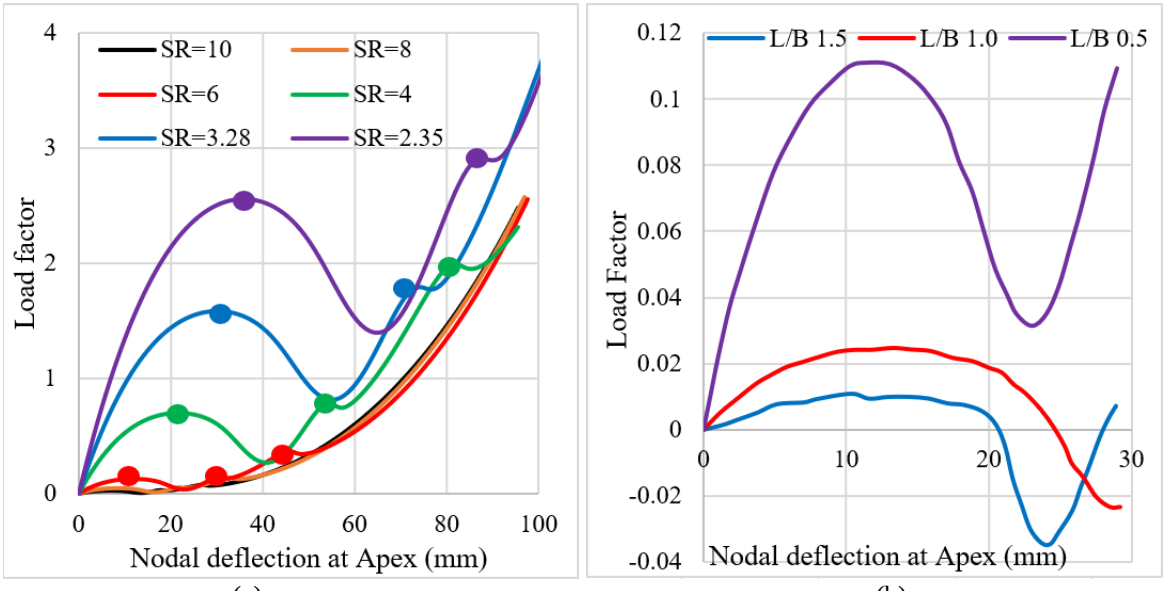

(a) (b)

Figure 6: (a) Load factor vs apex displacement of different span-to-rise ratios when Line Load applied, (b) Load factor vs apex displacement with varying L/B ratios with apex line load.

4.2 Effect of span-to-breadth (L/B) ratio

While investigating the influence of L/B ratio, an additional focus was to find whether there is a limiting L/B ratio above which there is no influence on the critical load. Fig 6(b) shows with apex line load for L/B ratios 0.5, 1.0 and 1.5 and Fig 7 is for uniform pressure loads for which typical snap-through are not seen. However, for L/B ratio of 0.5, i.e., breadth larger than span, the apex deflection is downward throughout the loading (in-set plot). For all span-to-rise ratios in Fig 8, a trend is seen typically between L/B ratios of 2.0-3.5 beyond which the L/B ratio has little effect on the critical load. For deeper barrel vaults (low span-to-rise) this L/B ratio is larger. This is because, for deeper vaults the transverse edges (along width) exhibit better participation in the load distribution until the occurrence of the snap-through.

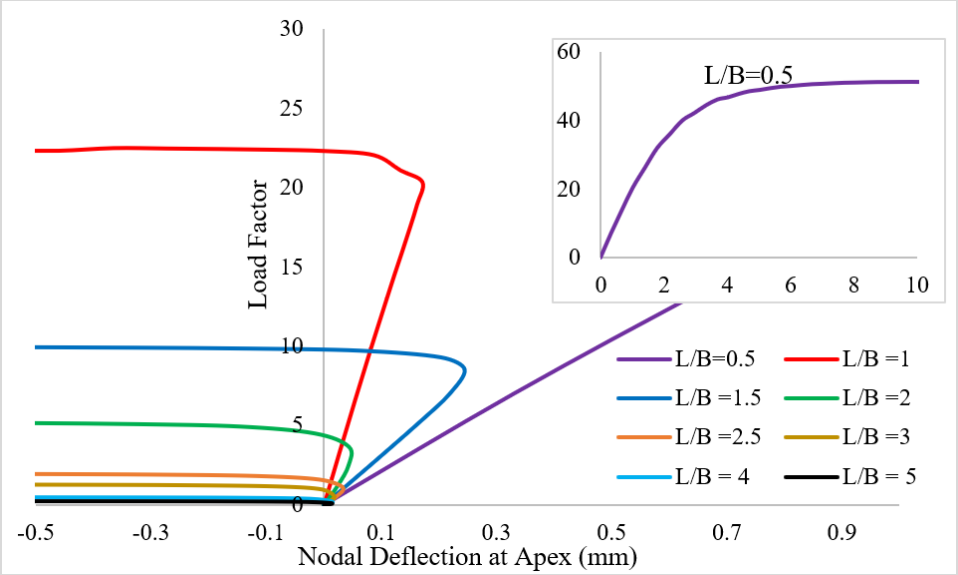

Figure 7: Effect of different L/B ratios in barrel vaults with uniform pressure

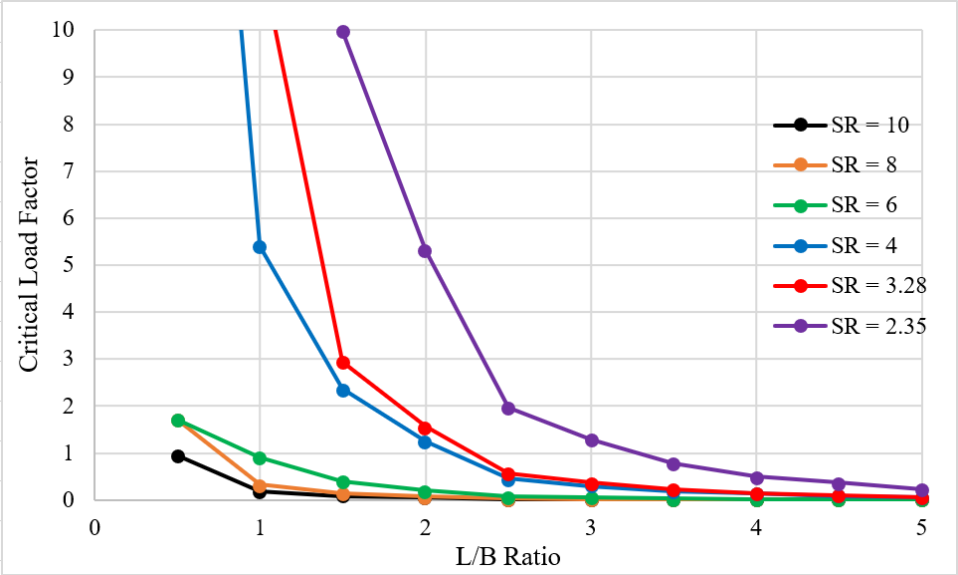

Figure 8: Variation of reticulated barrel vault stability limits based on geometric ratios with uniform pressure

The L/B ratio does not have any considerable influence on the critical load of shallow barrel vaults. From a practical consideration, adopting higher global safety factor would be sufficient for safeguarding against stability for such barrel vaults.

4.3 Post-buckling of Barrel Vaults under Wind Load distribution

All comparisons with uniform pressure are made under the condition that the total algebraic sum of all the nodal loads are equal between uniform pressure case and wind pressure case. This sum is distributed among the nodes of the barrel vault based on the net pressure coefficients applicable to that part of the barrel vault. Fig 9 shows a sample plot of load factor vs apex deflection under practical wind pressure for different cross-section areas of member. The wind pressure distribution is positive on the windward side and negative (uplift) on the central portion and leeward side (Fig 2). The load vs deflection response under this unsymmetric pressure seen from Fig 9 is uplift till the critical load after which the deflection follows back along a close path and continues downward deflection. To explain this, four points namely A, B, C and D have been marked on the curve of cross-section area 181 mm^2. Point A is at the origin of the curve i.e., undeflected position, point B is marked prior to the critical load where the apex node deflects upward. Point C is the critical load factor point until where the negative (upward) deflection continues. Point D is on positive deflection axis is located after the attainment of critical load. Fig 10 shows the deflected position of the apex node corresponding to load factors at points B and D, at the central cross-section of the vault highlighted by the dotted vertical plane.

The difference in response between uniform pressure and wind pressure distribution is shown in Fig 11(a) and Fig 11(b) respectively with L/B ratio and span-to-rise ratio. It is observed that the critical load under wind pressure distribution is always below that of uniform pressure for the same total loads. The difference however, will be based on the actual wind pressure coefficients, differing with elevation from the ground and curvature. For barrel vaults with lower span-to-rise ratio, this difference is larger since the negative pressure coefficients are larger. The critical load factor due to both cases tend to with both increasing L/B ratios and span-to-rise ratios. The in-set figures in Fig 11(a) and Fig 11(b) depict the curves at a closer scale. It was seen in the previous section that apex line loads and central concentrated loads led to significantly lower critical load factors than uniform pressure. Therefore, while wind pressure type load distribution is more critical than uniform pressure, it is still a remarkably more favourable load distribution than the former two load patterns. Hence, for practical purposes, it would be suitable to apply the uniform pressure case to find the critical load factors and then apply reductions to make the prediction applicable to wind pressure distribution.

4.4 Comparison of Results with Analytical Equations

Critical loads of reticulated vault have been calculated with the help of the solid cylindrical shell equations in literature and converting the cross-sectional area contributed by all members into an equivalent thickness for usage in these equations. Unfortunately, however, there is very little correspondence between the two literature based predictions and neither with the predictions of the post-buckling analysis. One reason can be attributed to the inclusion of flexural and axial terms in the equation by Timoshenko (2009) which is absent in that by Cheng and Ho (1963). While the Timoshenko occasionally coincides with the analysis prediction at low values of *Rt/L*, the Cheng and Ho (1963) predictions are about 1 order lower than the analysis predictions and 2 orders lower than the Timoshenko (2009) predictions. Evidently, the material averaging method

to evaluate an equivalent thickness for reticulated barrel vaults has not been successful in adapting the equations developed for solid barrel vaults. All the critical load factors have been converted into the critical pressure in Fig 12.

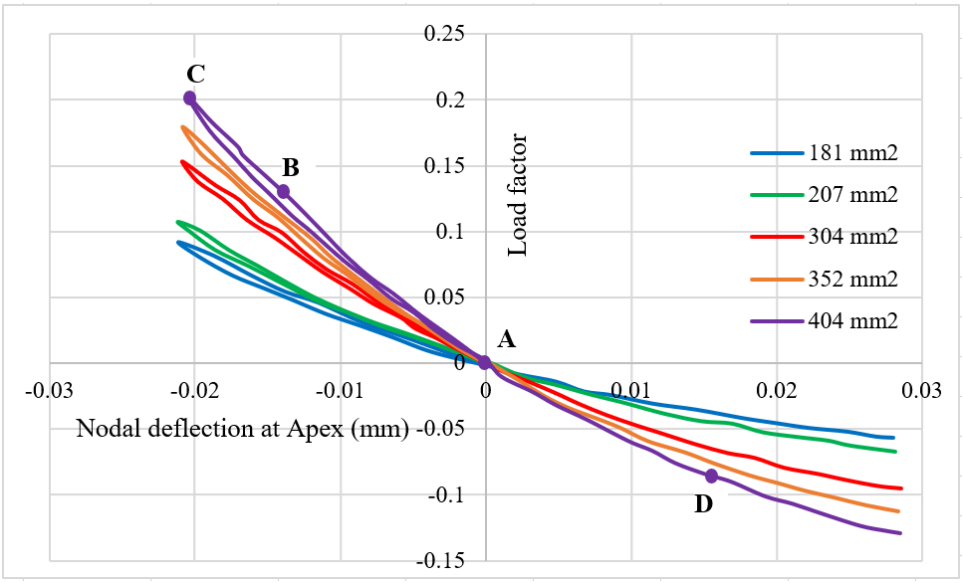

Figure 9: Load factor vs apex deflection for barrel vaults subjected to practical wind pressure

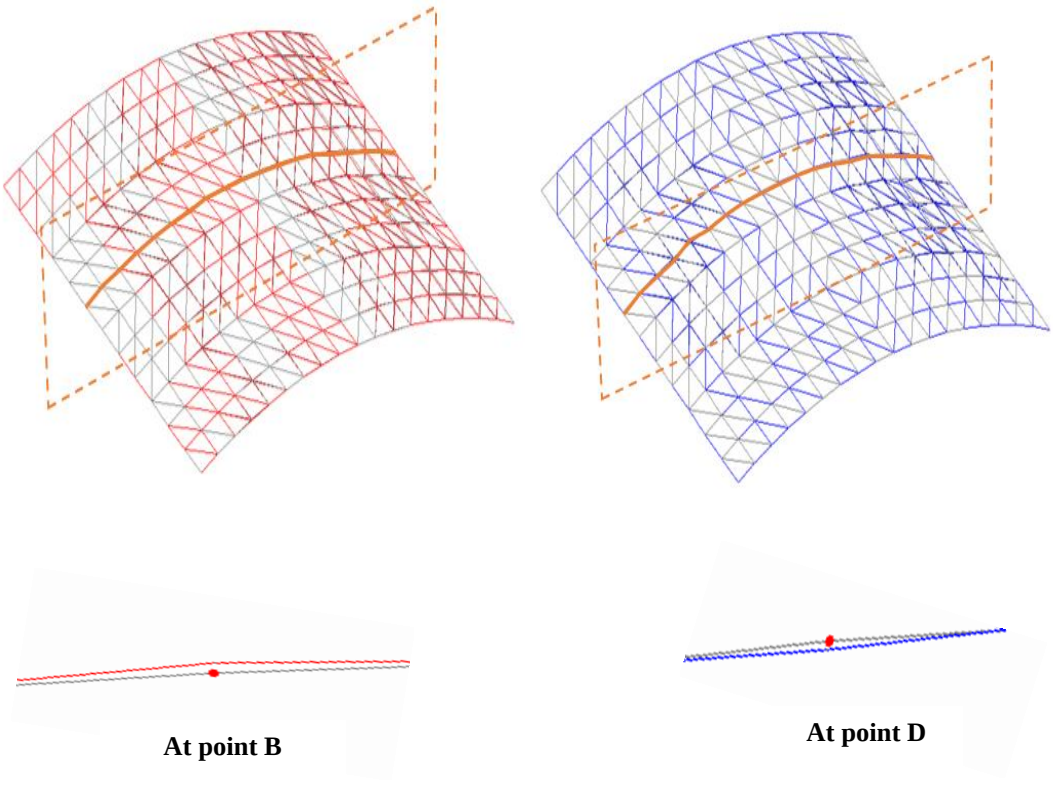

Figure 10: Deflected shape of barrel vault subjected to practical wind pressure

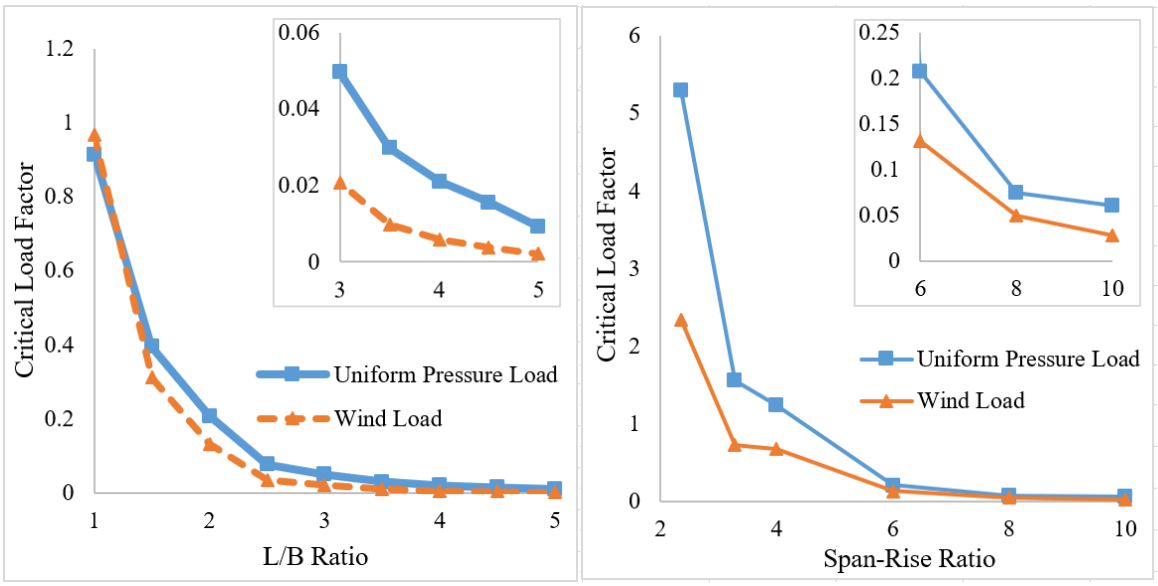

Figure 11: Sample variations of critical load factors with L/B ratio (shown for span-to-rise ratio of 6) and with span-to-rise ratio (shown for L/B ratio of 2.0).

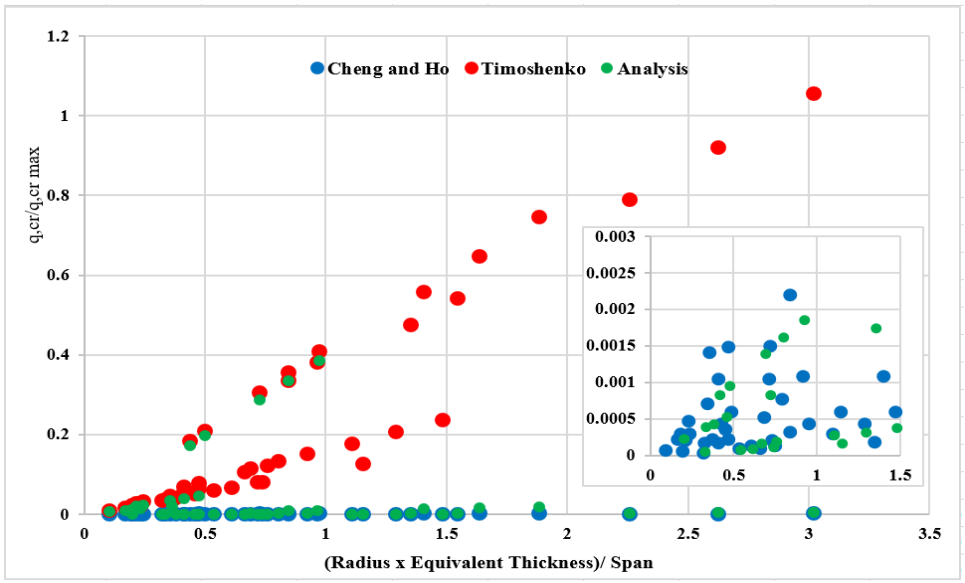

Figure 12: Comparison of results from analysis with available equations

5. Conclusions

In this study, the elastic post-buckling analysis of reticulated barrel vaults was conducted with varying geometric parameters and loading patterns. The corotated – updated Lagrangian formulation was used for performing the geometric nonlinear analysis. For practical interest, wind pressure distributions according to codebooks was also included for comparison of critical load predictions. The effect of the span-to-breadth and span-to-rise ratios with all the loading patterns were discussed. Finally, an attempt was made to evaluate existing critical load equations

in literature for solid barrel vaults with equivalent thickness modification. The conclusions drawn from the analysis performed in this study are summerised below:

1. Critical loads of the vaults subjected to ideal symmetric loads viz., concentrated central load, apex line load and uniform pressure load
    a. increase by the same percentage as the increase in the cross-sectional area of the members. The percentage increment of critical load is almost the same as the increment in member cross-section area.
    b. decreases with L/B ratio and after L/B ratio of 2.0-3.5, the L/B ratio has no significant effect on the critical load
    c. decreases with increase in span-to-rise ratio which is more pronounced at lower span-to-rise ratios. Above ratio of 6, the critical load factors reductions are comparatively lower.
2. The attempt to apply equations in literature for solid cylindrical shells to reticulated barrel vaults were unsuccessful. They show no correspondence with each other or with the post-buckling analysis predictions. The predictions by the various equations are 1-2 orders different from the analysis predictions. The adoption of an equivalent thickness for the application of these equations to reticulated barrel vaults did not help in improving these.
3. Vaults subjected to uniform pressure have the highest critical loads among the 3 ideal load patterns for the same total load magnitude. Wind pressure distribution which is unsymmetric and consisting of both uplift and downward pressures is more critical than uniform pressure but still considerably safer than line load or concentrated loads since the pressure is still distributed on all nodes of the barrel vault.
4. Post-buckling curves of barrel vaults subjected to concentrated central load and apex line load follows the familiar post-buckling path where critical load is attained followed by snap-through buckling. The post-buckling curve under uniform pressure undergoes deflection reversal after the critical load while for wind pressure, the post-buckling curve is one of uplift till the critical point followed by reversal along the same path and downward deflection. However, this curve shape may depend on the wind pressure coefficients and curvature.
5. The critical load of barrel vaults subjected to wind pressure exhibits the same behavior with respect to changes in L/B ratio and span-to-rise ratio as those subjected to uniform pressure. Due to close resemblance of post-buckling behavior and lower difference in critical load (compared to the other two load patterns) the uniform pressure case can be used along with some reduction factors to estimate critical load under wind pressure.

References

Ahmadizadeh M., Maalek S. (2014). "An investigation of the effects of socket joint flexibility in space structures." *Journal of Constructional Steel Research*, 102, 72-81.

Chan, S. L. (1988). "Geometric and material non-linear analysis of beam-columns and frames using the minimum residual displacement method." *International Journal for Numerical Methods in Engineering*, 26(12), 2657-2996.

Cheng, S., Ho, B. P. C. (1963). "Stability of Heterogeneous Aeolotropic Cylindrical Shells under Combined Loading." *Journal of American Institute of Aeronautics and Astronautics* , 1(4), 892-898.

Dara, P., Ramalingam, R., Kumar, G.K. (2020). "Post-buckling strength of single layer domes under distributed loading." *Proceedings of Annual Stability Conference*, Structural Stability Research Council Atlanta, Georgia.

De Borst R., Crisfield, M. A. Remmers, J. J., Verhoosel, C. V. (2012). "Nonlinear finite element analysis of solids and structures.", John Wiley & Sons.

El-Sheikh, A. (1996). "Sensitivity of Space Trusses to Uneven Support Settlement." *International Journal of Space Structures*, 1(4), 392-400.

El-Sheikh, A. (1997). “Sensitivity of Space Trusses to Sudden Member Loss.” *International Journal of Space Structures*, 12(1), 31-41.
El-Sheikh, A. (2001). “Effect of Geometric Imperfections on Single-Layer Barrel Vaults.” *International Journal of Space Structures*, 17(4), 271-283.
Hill, C.D., Blandford, G.E., and Wang, S.T. (1989). “Post-buckling analysis of space steel truss.” *Journal of Structural Engineering*, 115(4), 900-919.
Jayachandran, S.A., Kalyanaraman, V., Narayanan, R. (2003). “A co-rotation-based secant matrix procedure for elastic post buckling analysis of truss structures.” *International Journal of Structural Stability and Dynamics*, 4(01),1-19
Jeyabalan, A.K., Ramalingam, R. (2021). “Sensitivity of post-buckling behaviour of single layer reticulated shells to loading and member imperfections” *Proceedings of Annual Stability Conference*, Structural Stability Research Council, Denver, Colorado.
Lopez, A., Puente, I., Serna, M.A. (2007). “Numerical model and experimental tests on single-layer latticed domes with semi-rigid joints.” *Computers and Structures*, 85, 360–374.
Lo Frano, R., Forasassi, G. (2008). “Buckling of imperfect thin cylindrical shell under lateral pressure.” *Science and Technology of Nuclear Installations*, 2008.
Ma, H., Fan, F., Wen, P., Zhang, H., Shen, S. (2015). “Experimental and numerical studies on a single-layer cylindrical reticulated shell with semi-rigid joints.” *Thin-Walled Structures*, 86, 1–9.
Mattiasson, K. (1983). “On the corotational finite element formulation for large deformation problems.” Doctoral Thesis, Chalmers University of Technology, Sweden.
Mohit, M., Sharif, Y., Tavakoli, A. (2020). “Geometrically nonlinear analysis of space trusses using new iterative techniques.” *Asian Journal of Civil Engineering*, 21, 785–795.
Niea, G., Xiao, C., Zhic, X.D. (2017). “Damage quantification, damage limit state criteria and vulnerability analysis for single-layer reticulated shell.” *Thin-walled structures*, 120, 378-385.
Pajand, M.R., Alamatian, J. (2011). “Automatic DR structural analysis of snap through and snap back using optimized load increment.” *Journal of Computing in Civil Engineering*, ASCE, 137(1), 325-335.
Papadrakakis, M. (1983). “Inelastic Post-Buckling Analysis of Trusses.” *Journal of Structural Engineering*, ASCE, 109(9), 2129-2147.
Ramalingam, R., Jayachandran, S.A. (2015). “Post buckling behaviour of flexibly connected single layer steel domes.” *Journal of Constructional Steel Research*, 114, 136-145.
Roudsari, M.T., Gordini, M., Fazeli, H., Kavehei, B. (2017). “Probability Analysis of Double Layer Barrel Vaults Considering the Effect of Initial Curvature and Length Imperfections Simultaneously.” *International Journal of Steel Structures*, 17(3), 939-948.
Sheidaii, M.R., Bayrami, S., Babaei, M. (2013). “Collapse Behavior of Single-Layer Space Barrel Vaults under Non-Uniform Support Settlements”, *International Journal of Steel Structures*, 13(4), 723-730.
Thai, H.T., Kim, S.E. (2009). “Large deflection inelastic analysis of space trusses using generalized displacement control method” *Engineering Structures*, 126(4), 738-749.
Timoshenko, S. P., Gere, J. M. (2009). “Theory of elastic stability.” *McGraw Hill Education (India) Edition*, New Delhi.
Ya, J., Qin, F., Cao, Z., Fan, F., Mod, Y.L. (2016). “Mechanism of coupled instability of single-layer reticulated domes.” *Engineering Structures*, 114, 158–170.
Yang, Y.B., Yang, C.T. (1996). “Effects of member buckling and yielding on ultimate strengths of space trusses.” *Engineering Structures*, 19(2), 179-191.
Xiong, Z., Guo, X., Luo, Y., Zhu, S., Liu, Y. (2017). “Experimental and numerical studies on single-layer reticulated shells with aluminum alloy gusset joint.” *Thin-walled Structures*, 118, 124-136.